Journal of
Mechanical
Science and
Technology

Journal of Mechanical Science and Technology 21 (2007) 1456~1463

Finite element simulation of deformation processes of micro-components

W. M. Gao*, L. X. Kong and P. D. Hodgson

Centre for Material and Fibre Innovation, Deakin University, Geelong, VIC 3217, Australia

(Manuscript Received May 31, 2007; Revised August 30, 2007; Accepted September 30, 2007)

Abstract

The aim of this paper is to improve the understanding of deformation of micro medical needle and thread during assembly and then to develop an economical and flexible deformation method. Therefore, the swaging process is computationally simulated with the finite element method in this paper. A commercially available explicit nonlinear finite element analysis code, LS-Dyna, is used to model the 3-D deformation and contact problem. As the firmness of the assembly on the needle depends on the contact force and friction, the contact and the slide between the needle and thread are taken into account in the simulation. The general surface-to-surface contact algorithm (STS) is used to simulate the contact. The paper provides an insight into the deformation of the micro products.

Keywords: Assembly; Micro medical needle; Thread; Finite element method

1. Introduction

The assembly of medical needle with thread is an important process. A fast, precise and firm mount is generally required [1, 2]. The fixture that is widely used is a swaging jaw. Conventional jaw is fabricated from a pair of rigid parts each having a jaw at one end and a handle at the other end. Physician can squeeze the two handles together to cause the jaws to swage the needle end with a micro hole, where a thread was inserted in previously (Fig. 1). As a result, the needle and the thread are mounted together for suturing. Although the versatile and widespread method is easily operated, several problems have been found in practice. There is a need for the needle-thread assembly with an improved swaging jaws or a novel instrument which can overcome those problems. Medical needles and threads come in various sizes and are used for particular medical procedures [1, 3, 4]. Thus the jaw should be capable of tension adjustment to swage a variety of needles including.

To design a flexible swaging jaw, the swaging process must be studied systematically. The assembly of micro components includes not only deformation aspects but also friction due to contacts, which may occur throughout the whole process. To obtain a fast and firm assembly, the mechanical behaviour of needle and thread as well as the reactions both between the needle and thread and between the jaw and the needle should be included. The finite element (FE) method is a suitable tool to carry out parametric studies instead of manufacturing specimens and performing the measurements of parameters, which are difficult for micro-components [5-8]. Both the assembly reliability and the defects can be found from FE results, such as stress or strain concentrations or strain energy distributions. This paper computationally simulated the conventional jaw swaging process to investigate the deformation of both the needle and the thread responding to the press and finally to reveal the mysteries that cause those defect.

*Corresponding author. Tel.: +61 3 5227 2334 Fax.: +61 3 5227 1103
E-mail address: weimin.gao@deakin.edu.au

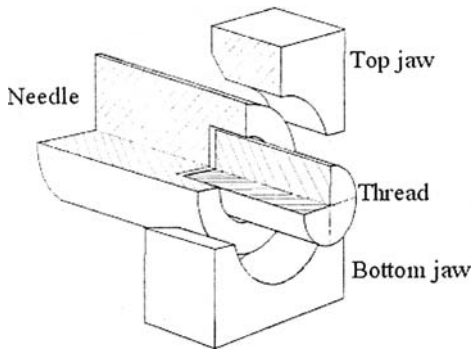

Fig. 1. Mechanism of assembly with swaging jaw.

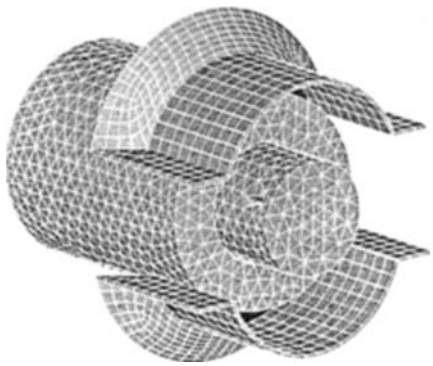

Fig. 2. Model of assembly.

2. Modelling

2.1 Model and swaging process

In the present work, the simulation was performed only for the conjunctive section, as shown in Fig. 2. The needle was fabricated by stainless steel 420 wire with a diameter of 0.56 mm. It has a hole of 0.318 mm in diameter and up to 0.4 mm deep at the end. A polyamide nylon thread of 0.3 mm in diameter was used. Each jaw has a shallow (less than semicircular) concavity. The radius of the concavity is 0.55 mm and the width is 1.52 mm.

The simulation was implemented with ANSYS-LS-DYNA [9]. The stainless steel component is assumed to be an elastic-plastic material, while a multi-linear elastic-plastic material model named "piecewise linear plasticity model" is used to describe the material properties of the polyamide nylon thread. The needle and the thread were meshed with hexahedral element (Solid 168). The jaws are considered as a rigid bodies and then the shell element of Shell 163 is used to mesh the surfaces of

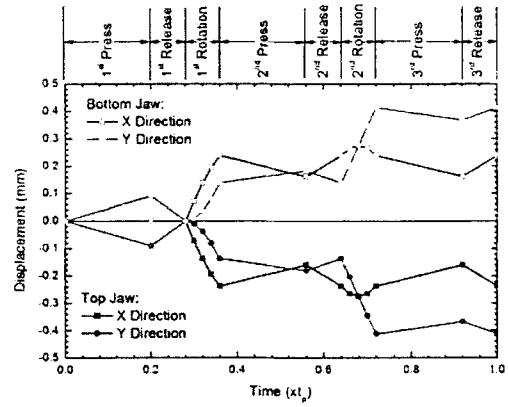

Fig. 3. The displacements of top and bottom jaws in the X and Y directions.

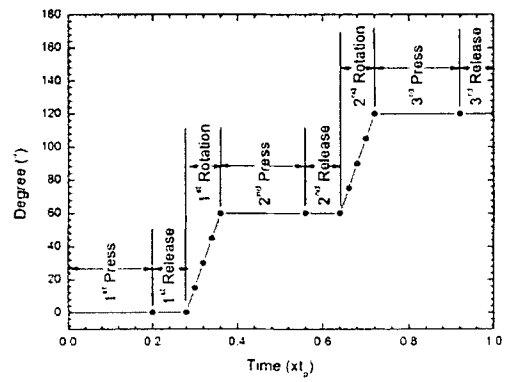

Fig. 4. The rotation of the top and bottom jaws.

the jaws. The ends of both the needle and the thread were free during swaging, i.e. no restriction was imposed on their boundaries.

The assembly is a three-step process as shown in Fig. 3. The swaging jaws firstly press the needle in the vertical direction (Y direction). The displacement was determined on that the final centres of the semicircular concavities of the top and bottom jaws share one point. After the first press, the jaws move back to their original positions and, then, rotate 60° clockwise (positive direction of Z) to be ready to second press (Fig. 4). Same pressing velocities were used for the three steps in the present work.

2.2. Contact modelling

The assembly of needle with thread is not only a frictional connection process but also an energy transfer process through contact surfaces. There are three contacts. In addition to the contacts between the

jaws and the needle and the contact between the circular surface of the inside hole of the needle and the outside circular surface of the thread, the contact between the disc surface of the needle hole and the disc end of the thread is also taken into account in the modelling, because the nylon thread may expand and reach to the needle when swaging, although there is an initial gap between the thread end and the needle. These contacts make the modelling of the assemble process very complex and time consuming.

The general surface-to-surface (STS) contact algorithm [9] is used for the above contacts, as the needle and thread have large deformation and experience large amounts of relative slide. For the jaw-needle contact, the jaws are defined as a target and the needle is assumed to be contact objects. For needle-thread contacts, the targets and contact objects are defined arbitrarily. The contact depth is assumed to be 1×10^{10} (nearly infinite), therefore, any time a contact node passes behind a target surface, contact is defined and a force is generated.

Friction plays a paramount role in the assembly process, especially, for the needle-thread, as the reliability of the assembly depends on the friction between them. Therefore, the slides between them are simulated in the computational model and friction is calculated for the contact surfaces. The frictional coefficient (μ_c) is determined from the static friction coefficient (μ_S), the dynamic friction coefficient (μ_D), the exponential decay coefficient (α), and the relative velocity, V_{rel}, of the surfaces in contact as expressed by Eq. (1):

$$\mu_c = \mu_D + (\mu_S - \mu_D)\exp(-\alpha|V_{rel}|) \quad (1)$$

In the present study, the static friction coefficient of 0.25 and the dynamic frication coefficient of 0.2 are used in the modelling for all contacts. Because the transition from static friction to dynamic friction is very sharp, the exponential decay coefficient should be a large value. In this work, a value of more than 8000 is used.

3. Results and discussion

Figs. 5-7 show the elastoplastic deformation and stress distribution in the needle and the thread during the three swaging steps, respectively.

As the concavity of jaws is less in radius than the needle, the press starts at the contact points between the corners of the mouth of jaws and the needle (Fig. 5 assembly-a) and the contacts gradually spread as the jaws move close, finally the jaws and the needle are in full engagement. This leads to the large movement of metal at the left and right regions in the needle and bulges were found in the compressed regions between either the left or the right ends of the top and the bottom jaws (Fig. 5 assembly-b and assembly-c). The formation of bulges not only results the consumption of swaging energy but also causes the unexpected formation of the needle. The bulges will increase when using a pair of jaws with smaller radius concavity to swage a needle with larger diameter. Thus a series of swaging jaws have to be designed for the needles used in different medical surgeries. Those needles are normally from 0.44 mm to 1.10 mm in diameter. To reduce the number of swaging jaws, an assembly method should be developed to use one flexible instrument for different sizes of needles.

The needle-thread contact and sequentially the deformation of the thread occur when there is an enough deformation of the needle, as the diameter of the thread is 0.018 mm smaller than the hole of the needle (Fig. 5 thread-a). Because the needle-thread connection is frictional, the solidity of the assembly depends on the contact area, the interaction between them and the deformed shape of the thread. In the present simulation, the width of the contact between the jaws and the needle, i.e., the distance from the end of the needle to the edge of the jaws, is 0.17 mm. The deformation of thread only takes place in a narrow region. Fig. 5 thread-b shows that the deformation area is only about 0.2 mm in width and the maximum compression is in the position where the thread contacts with the circular edge of the needle end. The stress focuses on the top and bottom narrow contact regions. As a result, the pull-out strength of the thread is reduced, even though the high stress regions disappear and the deformed surface of the thread becomes smoother after the second press (Fig. 6 thread-c and Fig. 7 thread-c).

The second and the third presses lead to the formation of a circular concavo-convex surface on the thread and also small circular convexities were found at both sides of the hollow (Fig. 7 thread a-c and Fig. 8). This structure increases the firmness of the assembly. An optimal shape of the thread may be formed and the formation of local high-stress regions that found in first press can be avoided by adjusting the pressing position. However, it is hard to locate the

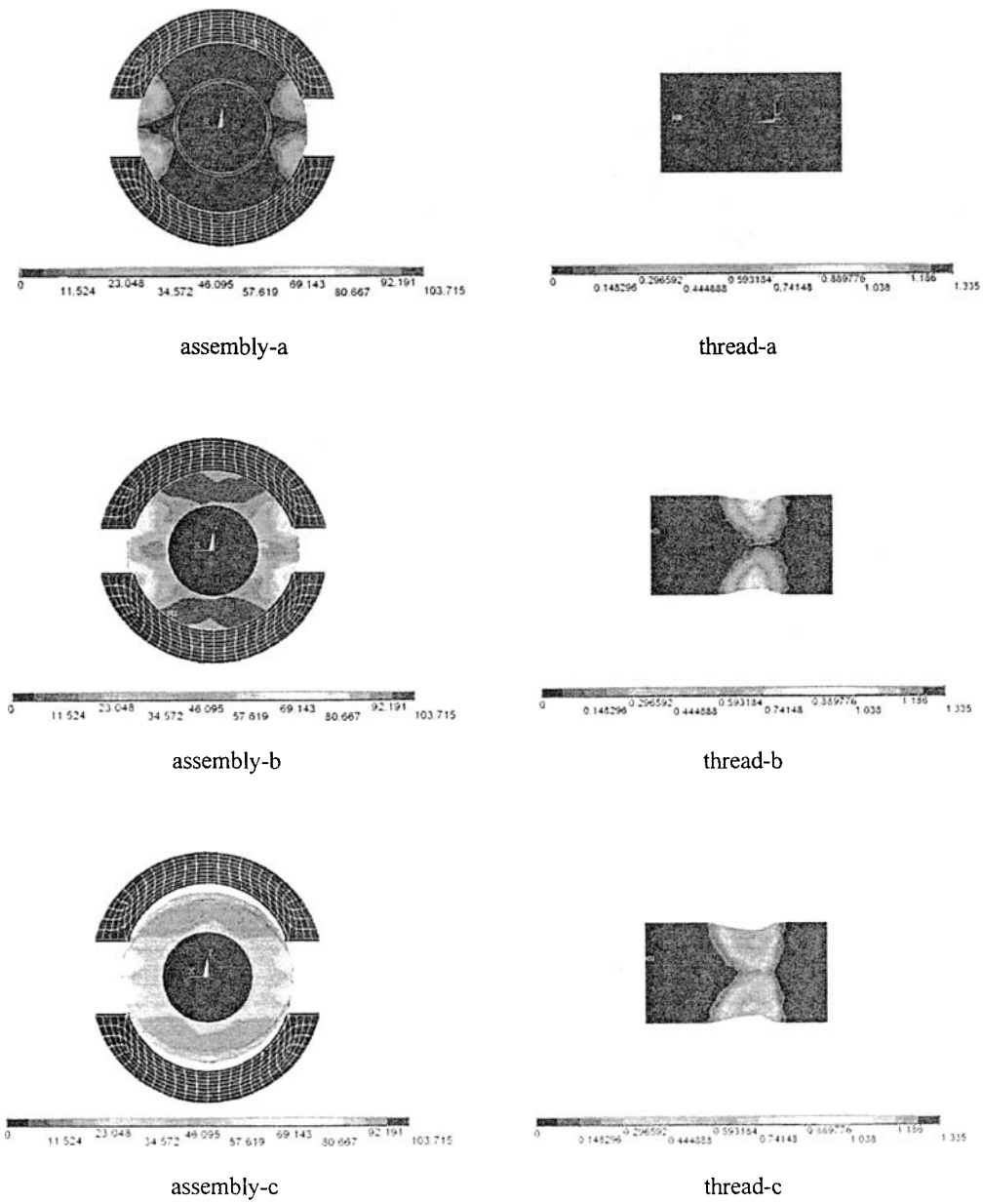

Fig. 5. Stress distribution on the needle and thread surfaces in the first press.

present kind of swaging jaws in a right pressing position. This is also one of the reasons that caused shortcomings of assembly.

As the swaging jaws were defined as a rigid body, the interaction between the jaws and the needle is represented by three force components corresponding to X, Y and Z directions, Fx, Fy and Fz. Because the pressing direction is changed twice, Fx and Fy cannot clearly present the interaction between the jaws and the needle. A normal force and a shear force were, therefore, derived from Fx and Fy with vector calculation. The force in the normal direction is defined as the pressing force of the swaging. Fig. 9 shows the variation of the pressing force during the three pressing steps. It can be seen that the contacts exhibit a complex mechanical behavior and nonlinear response, even in the elastic region of deformations, due to the interactions between the jaws and the

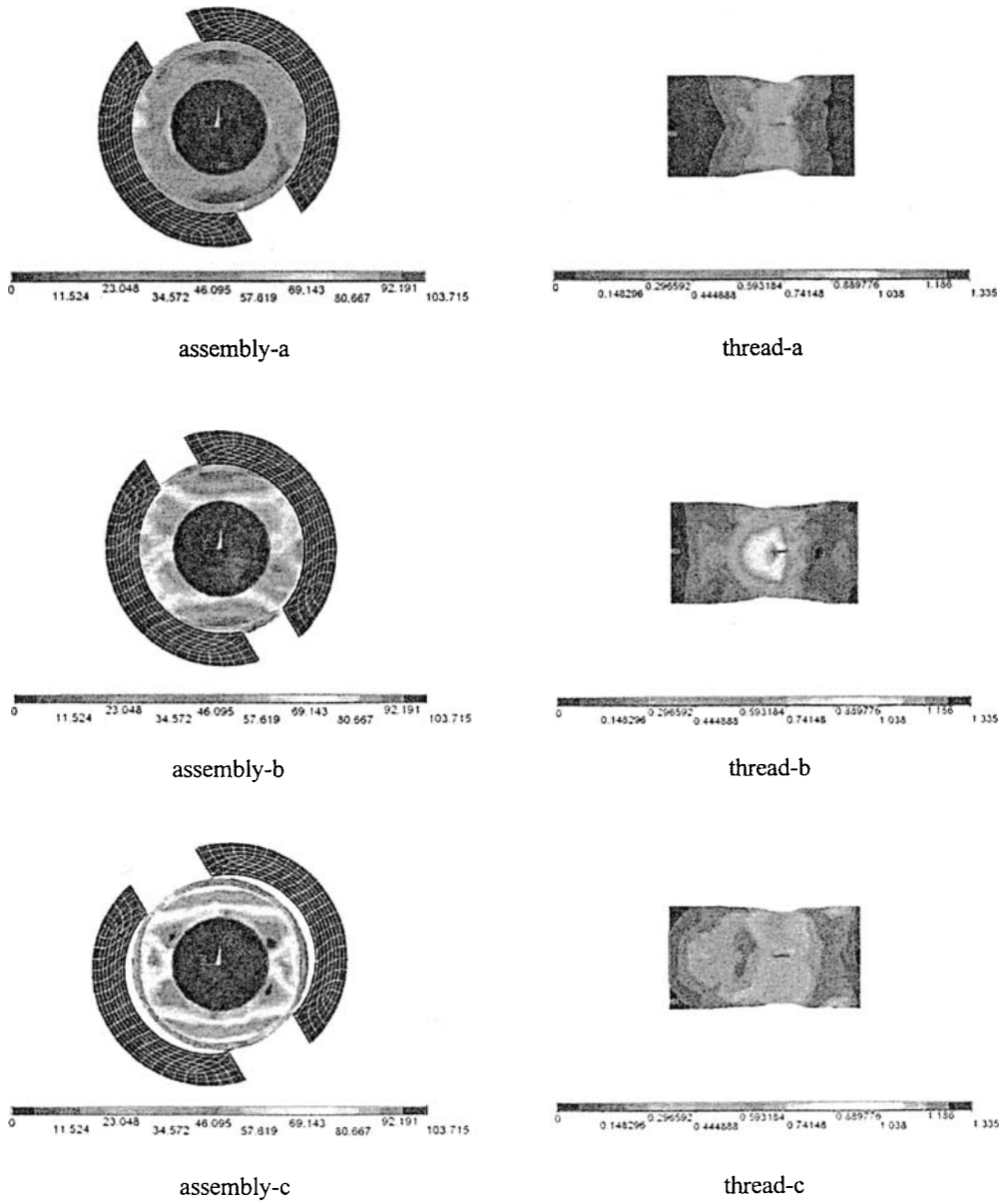

Fig. 6. Stress distribution on the needle and thread surfaces in the second press.

needle, not only the press but also the slide. It can be seen that the interaction force nonlinearly increases with the pressing depth of the jaws. The second deformation of the needle is much easier than the first one. The maximum required pressing force of the second press reduces to 7.5×10^3 N from 9.0×10^3 N of the first press. As the pressuring speeds are the same and a constant for the three press steps, the area between the force curve and x-axis in Fig. 9 is proportional to the work. The differences in area between different press steps imply that the required energy is significantly reduced step by step. The third press becomes not that important anymore to the formation of a wave-like circular surface, the smoothing of the needle surface and the increase of the firmness.

Fig. 10 shows the interaction between the needle and the thread. It can be seen that the needle-thread interaction is much complex than the jaw-needle contact. For the latter the interaction is dominated by

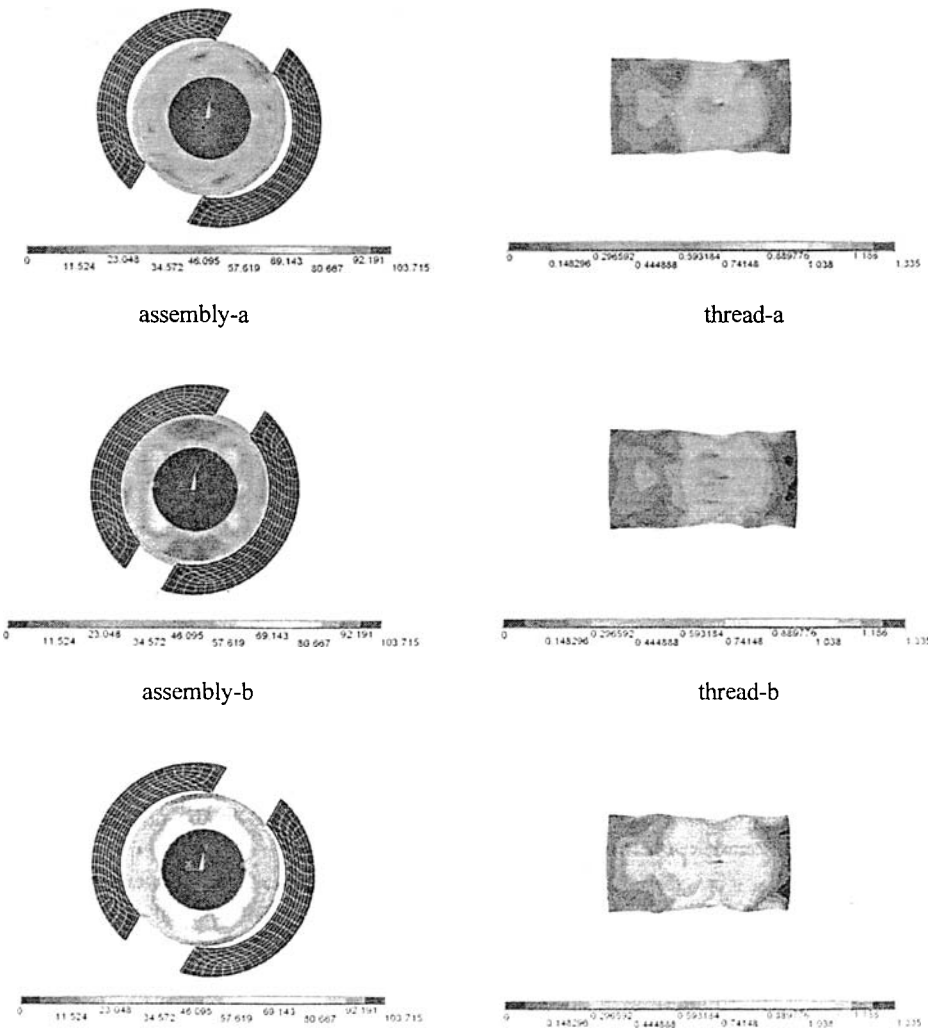

Fig. 7. Stress distribution on the needle and thread surfaces in the third press.

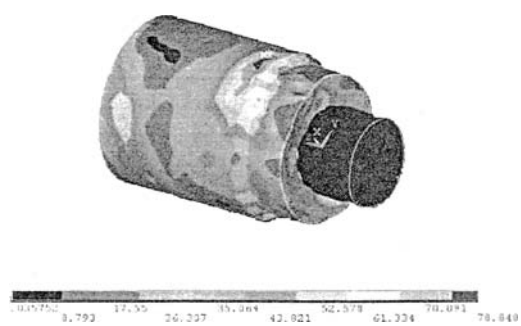

Fig. 8. The finial deformation and stress distribution of needle and thread.

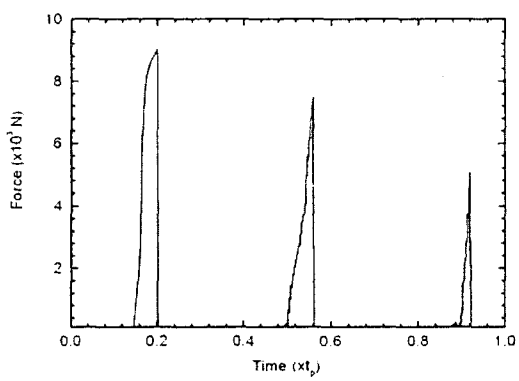

Fig. 9. The change of pressing force.

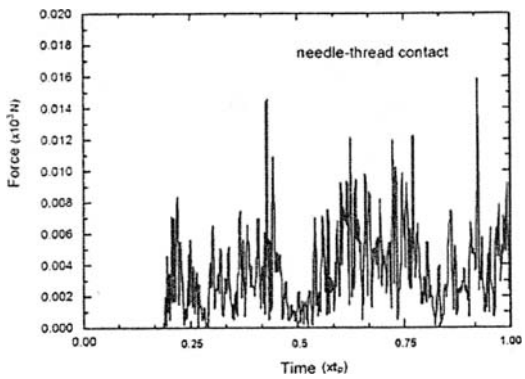

Fig. 10. Interaction between the needle and the thread.

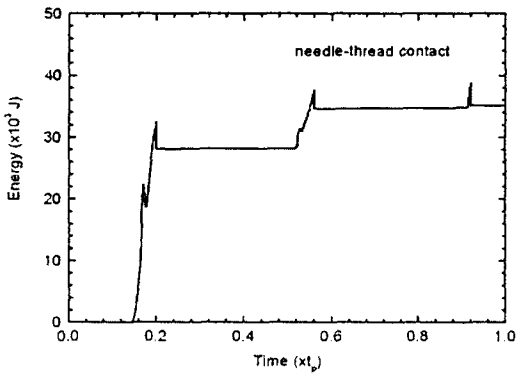

Fig. 11. The contact energy transferred between the needle and the thread.

the force in the pressing direction. The forces being vertical to pressing direction (except Z direction) are counteracted due to the opposition of their directions. The force in axial direction (Z-direction) is much smaller compared to other directions. For the former, however, the forces in the three directions are all important as the motion of nylon thread and the slide on the surface of the needle. Thus chaotic fluctuation was found for the needle-thread interaction force, which was calculated by a vector sum.

To clearly illustrate the interaction between the needle and the thread, a scalar quantity – contact energy was derived from the simulation results, as shown in Fig. 11. It can be seen that 80 % energy, which is referred to the total energy transferred through contact surface or the energy of the thread, is attributed to the first press. This suggests that the deformation of the thread in the first press is significant. With the progress of swaging, the deformation of the thread becomes smaller and smaller.

It can also be seen that there is a sharp decrease in the energy after each press step. This can be attributed to the spring of the compression due to the elastic characteristics. The energy is released in the defined "released step" in this paper. The released energies are approximately the same for the three steps. Fig. 11 also shows that almost all energy transferred into the thread in the third press is released. This suggests that the deformation of the thread is elastic and the third press is unnecessary. However, in practice, the imposed force either in the second press or in the third press is hard to be controlled manually.

4. Conclusions

The assembling process of a medical needle with a thread was simulated with the finite element method to improve the understanding of the process of swaging and the deformation characteristics both of the needle and thread. The advantages of the conventional assembling method and the shortcomings that may appear during swaging were analyzed based on the simulation results.

The simulation results show that the deformation of the needle and the thread exhibits a complex mechanical behavior. Large deformation exists in some local regions in the needle and the thread. A wave-like circular surface can be formed with the assembling method, which increases the firmness of the assembly. An optimal needle-thread contact structure can be created by changing the pressuring position. However, it is hard for the conventional assembling method due to its inherent limitations.

Acknowledges

This work was supported by the Australia Research Council (ARC LP0348045) and Dynek, which is highly acknowledged.

References

[1] Dynel PTY LTD, Dynek Sutures Global, (2006).
[2] Ethicon Inc., Control system for an automatic needle-Suture assembly and packaging machine, US 19980019138-19980206 (1998).
[3] Ethicon Inc., Automatic surgical needle and suture loading machine, US6014851 (2000).
[4] Ethicon Inc., System for needle thread putting and swaging, US19940181598 19940113 (1994)
[5] Y. Ansel, F. Schmitz, S. Kunz, H. P. Gruber, and G. Popovic, 2002, Development of tools for handling

and assembling micro-components, *Journal of Micromechanics and Microengineering.* 12 (2002) 430-437.

[6] B. Michel, J.-P. Sommer, V. Groβer: Application of fracture mechanics to micromechanics and micro system technology, *Advances in Fracture Research and Structural Integrity,* ed. V. V. Panasyuk et.al., Pergamon Press (1994) 683-690.

[7] K. Tsui, A. A. Geisberger, M. Ellis, G. D. Skidmore, Micro-machined end-effector and techniques for directed MEMS assembly, *J. Micromech. Microeng.* 14 (2004) 542-549.

[8] O. Nagler, M. Trost, B. Hillerich, F. Kozlowski, Efficient design and optimization of MEMS by integrating commercial simulation tools, *Sensors and Actuators.* A66 (1998) 15-20.

[9] Ansys Inc., ANSYS LS-DYNA User's Guide, (1997)